Title

Application of a metric for complex polynomials to bounded modification of planar Pythagorean-hodograph curves.

Authors

Farouki, Rida T

Knez, Marjeta

Vitrih, Vito

et al.

Publication Date

2024

Peer reviewed

Application of a metric for complex polynomials to bounded modification of planar Pythagorean–hodograph curves

Rida T. Farouki[1] Marjeta Knez[2,3] Vito Vitrih[4,5] Emil Žagar[2,3]

Abstract

By interpreting planar polynomial curves as complex–valued functions of a real parameter, an inner product, norm, metric function, and the notion of orthogonality may be defined for such curves. This approach is applied to the complex pre–image polynomials that generate planar Pythagorean–hodograph (PH) curves, to facilitate the implementation of bounded modifications of them that preserve their PH nature. The problems of bounded modifications under the constraint of fixed curve end points and end tangents, and of increasing the arc length of a PH curve by a prescribed amount, are also addressed.

Keywords: complex polynomial; inner product; norm; metric; Pythagorean–hodograph curves; bounded modification.

[1] Mechanical & Aerospace Engineering, University of California, Davis, CA 95616, USA
[2] Faculty of Mathematics and Physics, University of Ljubljana, Jadranska 19, Ljubljana, Slovenia
[3] Institute of Mathematics, Physics and Mechanics, Jadranska 19, Ljubljana, Slovenia
[4] Faculty of Mathematics, Natural Sciences and Information Technologies, University of Primorska, Glagoljaška 8, Koper, Slovenia
[5] Andrej Marušič Institute, University of Primorska, Muzejski trg 2, Koper, Slovenia

e–mail: farouki@ucdavis.edu, marjetka.knez@fmf.uni-lj.si, vito.vitrih@upr.si, emil.zagar@fmf.uni-lj.si

1 Introduction

In the complex model [4] for planar PH curves, points (x, y) in the Euclidean plane are identified with the complex values $x + \mathrm{i}\, y$. A planar PH curve $\mathbf{r}(t)$ for $t \in [\,0, 1]$ may be generated from a complex *pre–image polynomial* $\mathbf{w}(t)$ by integrating the hodograph expression $\mathbf{r}'(t) = \mathbf{w}^2(t)$. This guarantees that the components of $\mathbf{r}'(t) = x'(t) + \mathrm{i}\, y'(t)$ satisfy [13] the polynomial Pythagorean condition

$$x'^2(t) + y'^2(t) \;=\; \sigma^2(t)\,,$$

where $\sigma(t) = |\mathbf{r}'(t)| = |\mathbf{w}(t)|^2$ is the *parametric speed* of $\mathbf{r}(t)$ — the derivative $\mathrm{d}s/\mathrm{d}t$ of the curve arc length s with respect to the parameter t.

Planar PH curves admit an exact computation of properties such as arc lengths and offset curves [6], that necessitate use of numerical approximation for "ordinary" polynomial curves. However, their non–linear nature entails more sophisticated construction algorithms, and renders *a posteriori* shape modification a difficult task. To address this latter problem, it is important to first formulate a measure of "how close" two PH curves are, i.e., to specify a *metric* for the space of all planar PH curves.

The complex representation of planar PH curves offers a solution to this task, in terms of the standard concepts of inner products and norms from functional analysis [18]. By introducing a bound on the distance between an original and modified pre–image polynomial, it is possible to characterize the set of changes to its coefficients that define the shape modifications to a planar PH curve that do not compromise its PH nature.

The focus of the methodology presented herein is on the planar PH curves, although the approach may be adaptable to the spatial PH curves [3, 10] and the numerous other formulations of PH curves with distinctive properties that have been proposed [1, 2, 16, 17, 19, 20, 21, 22, 23, 24, 25].

The remainder of this paper is organized as follows. Section 2 introduces the basic concepts of an *inner product*, *norm*, and *metric* for the space of all polynomials in a real variable $t \in [\,0, 1\,]$ with complex coefficients. Section 3 then shows that this metric allows an *angle* between such polynomials to be defined, and gives examples of *orthogonal* plane curves specified as complex polynomial functions of a real parameter. Section 4 discusses the application of these concepts to planar PH curves and it is observed that to maintain the PH nature, modifications should be made to the pre-image polynomial instead of directly to the curve. Modifications satisfying a prescribed bound on the distance between the original and modified pre–image polynomials are discussed in Section 5, and modifications that preserve the end tangents or end points of PH curves are also formulated. Section 6 shows how complex polynomials orthogonal to a specified pre–image polynomial may be used to modify PH curve arc lengths. Finally, Section 7 summarizes the contributions of this study and suggests further possible avenues of investigation.

2 Metric space of complex polynomials

We begin by reviewing some elementary concepts from functional analysis — inner products, norms, and metrics (see [18] for a thorough treatment).

Let $\mathbf{u}(t), \mathbf{v}(t) \in \mathbb{C}[t]$ be complex polynomials in the real variable $t \in [\,0, 1\,]$. Their complex–valued *inner product* is defined by

$$\langle \mathbf{u}, \mathbf{v} \rangle \;=\; \int_0^1 \mathbf{u}(t)\, \overline{\mathbf{v}}(t)\; \mathrm{d}t\,. \tag{1}$$

For any complex polynomial $\mathbf{w}(t) \in \mathbb{C}[t]$, this inner product induces a non–negative norm specified by

$$\|\mathbf{w}\| \;=\; \sqrt{\langle \mathbf{w}, \mathbf{w} \rangle}\,. \tag{2}$$

A metric, or *distance function*, for the complex polynomials $\mathbf{u}(t)$ and $\mathbf{v}(t)$ may be defined in terms of the norm (2) as

$$\mathrm{distance}(\mathbf{u}, \mathbf{v}) \;=\; \|\mathbf{u} - \mathbf{v}\|\,. \tag{3}$$

Since

$$\begin{aligned} \|\mathbf{u} - \mathbf{v}\|^2 \;&=\; \int_0^1 (\mathbf{u}(t) - \mathbf{v}(t))(\overline{\mathbf{u}}(t) - \overline{\mathbf{v}}(t))\, \mathrm{d}t \\ &=\; \int_0^1 |\mathbf{u}(t)|^2 + |\mathbf{v}(t)|^2 - 2\,\mathrm{Re}(\mathbf{u}(t)\overline{\mathbf{v}}(t))\, \mathrm{d}t \\ &=\; \|\mathbf{u}\|^2 + \|\mathbf{v}\|^2 - 2\,\mathrm{Re}(\langle \mathbf{u}, \mathbf{v} \rangle)\,, \end{aligned}$$

we have

$$\mathrm{distance}(\mathbf{u}, \mathbf{v}) \;=\; \sqrt{\|\mathbf{u}\|^2 + \|\mathbf{v}\|^2 - 2\,\mathrm{Re}(\langle \mathbf{u}, \mathbf{v} \rangle)}\,.$$

Note that $\mathrm{distance}(\mathbf{u}, \mathbf{v}) = 0$ if and only if $\mathbf{u}(t) \equiv \mathbf{v}(t)$.

The metric (3) can be used to define the distance between planar curves, $\mathbf{r}(t)$ and $\mathbf{s}(t)$, regarded as complex functions of the real parameter $t \in [\,0, 1\,]$ — namely,

$$\mathrm{distance}(\mathbf{r}, \mathbf{s}) \;=\; \sqrt{\|\mathbf{r}\|^2 + \|\mathbf{s}\|^2 - 2\,\mathrm{Re}(\langle \mathbf{r}, \mathbf{s} \rangle)}\,.$$

Note that, when $\mathbf{r}(t)$ and $\mathbf{s}(t)$ are orthogonal, i.e., $\mathrm{Re}(\langle \mathbf{r}, \mathbf{s} \rangle) = 0$, the distance is simply $\sqrt{\|\mathbf{r}\|^2 + \|\mathbf{s}\|^2}$. The following elementary cases are noteworthy.

1. If $\mathbf{s}(t)$ is a translate of $\mathbf{r}(t)$ by the complex value $\mathbf{d}$, $\mathrm{distance}(\mathbf{r}, \mathbf{s}) = |\mathbf{d}|$.

2. If $\mathbf{s}(t)$ is a rotation of $\mathbf{r}(t)$ by angle θ, $\mathrm{distance}(\mathbf{r}, \mathbf{s}) = 2\,(1 - \cos\theta)\,\|\mathbf{r}\|$.

3. If $\mathbf{s}(t)$ is a scaling of $\mathbf{r}(t)$ by the factor c, distance$(\mathbf{r},\mathbf{s}) = |1-c\,|\,\|\mathbf{r}\|$.

In some contexts it may be desirable for distance$(\mathbf{r},\mathbf{s})$ to reflect only the differences of *shape*, and discount considerations of position, orientation, and scaling. If $\mathbf{r}(0) = \mathbf{s}(0) = 0$, this can be achieved through a rotation/scaling transformation that makes the vectors $\mathbf{r}(1) - \mathbf{r}(0)$ and $\mathbf{s}(1) - \mathbf{s}(0)$ coincident.

The preceding ideas were briefly mentioned in the problem of constructing spatial C^2 closed loops with prescribed arc lengths using PH curves [11] — the solutions can be characterized in terms of two complex polynomials $\mathbf{u}(t), \mathbf{v}(t)$ satisfying $\|\mathbf{u}\| = \|\mathbf{v}\| = 1/\sqrt{2}$, $\langle \mathbf{u}, \mathbf{v} \rangle = 0$, and thus distance$(\mathbf{u},\mathbf{v}) = 1$.

3 Orthogonal planar curves

Since $|\,\mathrm{Re}(\langle \mathbf{u}, \mathbf{v} \rangle)\,| \le \|\mathbf{u}\|\,\|\mathbf{v}\|$ from the Cauchy–Schwartz inequality, an angle $\theta \in [\,0, \pi\,]$ between $\mathbf{u}$ and $\mathbf{v}$ may be defined by

$$\cos\theta \;=\; \frac{\mathrm{Re}(\langle \mathbf{u}, \mathbf{v} \rangle)}{\|\mathbf{u}\|\,\|\mathbf{v}\|}\,,$$

and we thereby obtain the cosine rule

$$\mathrm{distance}^2(\mathbf{u},\mathbf{v}) \;=\; \|\mathbf{u}\|^2 + \|\mathbf{v}\|^2 - 2\,\|\mathbf{u}\|\,\|\mathbf{v}\|\cos\theta\,.$$

If $\cos\theta = 0$ — i.e., $\mathrm{Re}(\langle \mathbf{u}, \mathbf{v} \rangle) = 0$ — we say that $\mathbf{u}$ and $\mathbf{v}$ are *orthogonal*, and write $\mathbf{u} \perp \mathbf{v}$. For two orthogonal complex polynomials, the distance becomes simply $\sqrt{\|\mathbf{u}\|^2 + \|\mathbf{v}\|^2}$.

Although the focus herein is on PH curves, the above principles apply to *any* planar curves represented as complex-valued polynomial functions of a real variable, an approach to the study of planar curves promoted by Zwikker [27]. If $\mathbf{r}(t)$ and $\mathbf{s}(t)$ are Bézier curves of degree m and n, with control points $\mathbf{p}_0, \ldots, \mathbf{p}_m$ and $\mathbf{q}_0, \ldots, \mathbf{q}_n$, the product $\mathbf{r}(t)\,\overline{\mathbf{s}}(t)$ can be expressed [7] as

$$\mathbf{r}(t)\,\overline{\mathbf{s}}(t) \;=\; \sum_{k=0}^{m+n} \mathbf{z}_k \binom{m+n}{k} (1-t)^{m+n-k} t^k\,,$$

with

$$\mathbf{z}_k \;=\; \sum_{j=\max(0,k-n)}^{\min(m,k)} \frac{\binom{m}{j}\binom{n}{k-j}}{\binom{m+n}{k}}\,\mathbf{p}_j\,\overline{\mathbf{q}}_{k-j}\,, \quad k = 0, \ldots, m+n\,.$$

Since the definite integral of every Bernstein basis function of degree $m+n$ over $[\,0,1\,]$ is simply $1/(m+n+1)$, the inner product of $\mathbf{r}(t)$ and $\mathbf{s}(t)$ is

$$\langle \mathbf{r}, \mathbf{s} \rangle \;=\; \frac{\mathbf{z}_0 + \cdots + \mathbf{z}_{m+n}}{m+n+1}\,.$$

Thus, for given control points $\mathbf{p}_0, \ldots, \mathbf{p}_m$ of $\mathbf{r}(t)$, the orthogonality condition $\mathrm{Re}(\langle \mathbf{r}, \mathbf{s} \rangle) = 0$ amounts to a single linear constraint on the real and imaginary parts of the control points $\mathbf{q}_0, \ldots, \mathbf{q}_n$ of $\mathbf{s}(t)$, so the dimension of the subspace of degree n curves $\mathbf{s}(t)$ that are orthogonal to $\mathbf{r}(t)$ is $2\,n+1$. To explore this subspace in more detail, we set

$$(r_x(t), r_y(t)) \;=\; (\mathrm{Re}(\mathbf{r}(t)), \mathrm{Im}(\mathbf{r}(t)))\,, \quad (s_x(t), s_y(t)) \;=\; (\mathrm{Re}(\mathbf{s}(t)), \mathrm{Im}(\mathbf{s}(t)))\,,$$

and define

$$\begin{aligned} d(t) \;&:=\; \mathrm{Re}(\mathbf{r}(t)\,\overline{\mathbf{s}}(t)) \;=\; r_x(t)s_x(t) + r_y(t)s_y(t)\,, \\ c(t) \;&:=\; \mathrm{Im}(\mathbf{r}(t)\,\overline{\mathbf{s}}(t)) \;=\; s_x(t)r_y(t) - s_y(t)r_x(t)\,. \end{aligned}$$

Regarding $\mathbf{r}(t), \mathbf{s}(t)$ as vector functions, $d(t)$ is their dot product and $c(t)$ is the component of the cross product orthogonal to the (x,y) plane. Moreover, $\mathrm{Re}(\langle \mathbf{r}, \mathbf{s} \rangle)$ and $\mathrm{Im}(\langle \mathbf{r}, \mathbf{s} \rangle)$ are the integrals of $d(t)$ and $c(t)$ over $t \in [\,0,1\,]$.

To construct orthogonal curves, it is convenient to employ an orthonormal polynomial basis. We choose here the Legendre basis on $t \in [\,0,1\,]$ which may be expressed in terms of the Bernstein basis [5] as

$$L_k(t) \;=\; \sqrt{2k+1}\,\sum_{i=0}^{k} (-1)^{k+i} \binom{k}{i}\, b_i^k(t)\,, \quad b_i^k(t) \;=\; \binom{k}{i} (1-t)^{k-i} t^i\,.$$

These basis functions satisfy

$$\int_0^1 L_j(t) L_k(t)\;\mathrm{d}t \;=\; \delta_{jk}\,,$$

where δ_{jk} is the Kronecker delta, and the first few instances are

$$\begin{aligned} L_0(t) \;&=\; 1\,, \\ L_1(t) \;&=\; \sqrt{3}\,(2\,t-1)\,, \\ L_2(t) \;&=\; \sqrt{5}\,(6\,t^2 - 6\,t + 1)\,, \\ L_3(t) \;&=\; \sqrt{7}\,(20\,t^3 - 30\,t^2 + 12\,t - 1)\,. \end{aligned}$$

For any given curve $\mathbf{r}(t),\ t \in [\,0,1\,]$ of degree m we consider the problem of constructing curves $\mathbf{r}_\perp(t)$, of the same degree, that are orthogonal to $\mathbf{r}(t)$. Expressing $\mathbf{r}(t)$ and $\mathbf{r}_\perp(t)$ in the Legendre basis as

$$\begin{aligned}\mathbf{r}(t) \;&=\; \sum_{k=0}^{m} a_{k,1} L_k(t) \;+\; \mathrm{i} \sum_{k=0}^{m} a_{k,2} L_k(t)\,,\\ \mathbf{r}_\perp(t) \;&=\; \sum_{k=0}^{m} b_{k,1} L_k(t) \;+\; \mathrm{i} \sum_{k=0}^{m} b_{k,2} L_k(t)\,,\end{aligned} \tag{4}$$

by the orthonormality of the basis functions we have

$$\begin{aligned}\mathrm{Re}(\langle \mathbf{r}, \mathbf{r}_\perp \rangle) \;&=\; \int_0^1 \sum_{k=0}^{m} a_{k,1} L_k(t) \sum_{\ell=0}^{m} b_{\ell,1} L_\ell(t) + \sum_{k=0}^{m} a_{k,2} L_k(t) \sum_{\ell=0}^{m} b_{\ell,2} L_\ell(t)\,\mathrm{d}t\\ &=\; \sum_{k=0}^{m} a_{k,1} b_{k,1} + a_{k,2} b_{k,2}\,.\end{aligned}$$

Thus, identifying the coefficients $b_{k,1} + \mathrm{i}\, b_{k,2},\ k = 0, 1, \ldots, m$ of an orthogonal curve is equivalent to finding the set of $2m+1$ linearly independent vectors

$$\boldsymbol{b} \;=\; (b_{0,1}, b_{0,2}, b_{1,1}, b_{1,2}, \ldots, b_{m,1}, b_{m,2})^T \in \mathbb{R}^{2m+2}$$

that are orthogonal to the vector

$$\boldsymbol{a} \;=\; (a_{0,1}, a_{0,2}, a_{1,1}, a_{1,2}, \ldots, a_{m,1}, a_{m,2})^T \in \mathbb{R}^{2m+2}$$

with respect to the Euclidean inner (or dot) product in $\mathbb{R}^{2m+2}$. The basis of the orthogonal complement $\boldsymbol{a}^\perp$ follows from the extended QR decomposition $\boldsymbol{a} = QR$, where Q is a $(2m+2) \times (2m+2)$ orthogonal matrix, and $R = (\|\boldsymbol{a}\|_2\,, 0, \ldots, 0)^T$ where $\|\cdot\|_2$ is the standard Euclidean norm. The matrix Q is the well–known Householder reflection [15], computed as

$$Q \;=\; I - \frac{2}{\boldsymbol{g}^T\boldsymbol{g}}\,\boldsymbol{g}\boldsymbol{g}^T\,, \quad \boldsymbol{g} \;=\; \boldsymbol{a} + \mathrm{sign}(a_{0,1})\,\|\boldsymbol{a}\|_2\,\boldsymbol{e}_1\,, \tag{5}$$

where $\boldsymbol{e}_1 = (1, 0, \ldots, 0)^T$. The second through last columns of Q — denoted by $\boldsymbol{q}_2, \ldots, \boldsymbol{q}_{2m+2}$ — are the orthogonal basis of $\boldsymbol{a}^\perp$. Thus, any vector

$$\boldsymbol{b} \;=\; \sum_{k=2}^{2m+2} \xi_{k-1} \boldsymbol{q}_k\,, \quad \xi_1, \ldots, \xi_{2m+1} \in \mathbb{R}$$

identifies a curve $\mathbf{r}_\perp(t)$ of the form (4), that is orthogonal to $\mathbf{r}(t)$. Moreover, the columns of Q also define curves that are pairwise orthogonal.

Example 1. Consider the vector $\boldsymbol{a} = (\alpha_0, 0, 0, \alpha_1, \alpha_2, 0, 0, \alpha_3)$ that defines the curve

$$\mathbf{r}(t) \;=\; \alpha_0 L_0(t) + \alpha_2 L_2(t) + \mathrm{i}\,(\alpha_1 L_1(t) + \alpha_3 L_3(t))\,,$$

with Bézier control points

$$\mathbf{p}_0 \;=\; \alpha_0 + \sqrt{5}\,\alpha_2 - \mathrm{i}\,(\sqrt{3}\,\alpha_1 + \sqrt{7}\,\alpha_3) \;=\; \overline{\mathbf{p}}_3\,,$$

$$\mathbf{p}_1 \;=\; \alpha_0 - \sqrt{5}\,\alpha_2 - \mathrm{i}\,\left(\frac{\alpha_1}{\sqrt{3}} - 3\sqrt{7}\,\alpha_3\right) \;=\; \overline{\mathbf{p}}_2\,.$$

In this case, we obtain

$$Q = \begin{bmatrix}
-\frac{\alpha_0}{\alpha} & 0 & 0 & -\frac{\alpha_1}{\alpha} & -\frac{\alpha_2}{\alpha} & 0 & 0 & -\frac{\alpha_3}{\alpha} \\
0 & 1 & 0 & 0 & 0 & 0 & 0 & 0 \\
0 & 0 & 1 & 0 & 0 & 0 & 0 & 0 \\
-\frac{\alpha_1}{\alpha} & 0 & 0 & 1 - \frac{\alpha_1^2}{\alpha^2+\alpha_0\alpha} & -\frac{\alpha_1\alpha_2}{\alpha^2+\alpha_0\alpha} & 0 & 0 & -\frac{\alpha_1\alpha_3}{\alpha^2+\alpha_0\alpha} \\
-\frac{\alpha_2}{\alpha} & 0 & 0 & -\frac{\alpha_1\alpha_2}{\alpha^2+\alpha_0\alpha} & 1 - \frac{\alpha_2^2}{\alpha^2+\alpha_0\alpha} & 0 & 0 & -\frac{\alpha_2\alpha_3}{\alpha^2+\alpha_0\alpha} \\
0 & 0 & 0 & 0 & 0 & 1 & 0 & 0 \\
0 & 0 & 0 & 0 & 0 & 0 & 1 & 0 \\
-\frac{\alpha_3}{\alpha} & 0 & 0 & -\frac{\alpha_1\alpha_3}{\alpha^2+\alpha_0\alpha} & -\frac{\alpha_2\alpha_3}{\alpha^2+\alpha_0\alpha} & 0 & 0 & 1 - \frac{\alpha_3^2}{\alpha^2+\alpha_0\alpha}
\end{bmatrix},$$

where $\alpha = \|\boldsymbol{a}\|_2$. From columns $2, 3, 6, 7$, we see that any curve of the form

$$\mathbf{r}_\perp(t) \;=\; \beta_1 L_1(t) + \beta_3 L_3(t) + \mathrm{i}\,(\beta_0 L_0(t) + \beta_2 L_2(t)) \tag{6}$$

is orthogonal to $\mathbf{r}(t)$. The Bézier control points of such a curve are

$$\mathbf{q}_0 \;=\; -\sqrt{3}\,\beta_1 - \sqrt{7}\,\beta_3 + \mathrm{i}\,(\beta_0 + \sqrt{5}\,\beta_2) \;=\; -\,\overline{\mathbf{q}}_3\,,$$

$$\mathbf{q}_1 \;=\; -\frac{\beta_1}{\sqrt{3}} + 3\sqrt{7}\,\beta_3 + \mathrm{i}(\beta_0 - \sqrt{5}\,\beta_2) \;=\; -\,\overline{\mathbf{q}}_2\,.$$

Columns $4, 5, 8$ of Q define three additional linearly–independent orthogonal curves, that are symmetric about the real axis.

As an illustrative example, consider the case

$$\alpha_0 = 1,\ \alpha_1 = -2\sqrt{3},\ \alpha_2 = \sqrt{5},\ \alpha_3 = \sqrt{7}.$$

Figure 1 shows the curve $\mathbf{r}(t)$ (black) and four curves $\mathbf{r}_\perp(t)$ orthogonal to it, corresponding to the columns 4 (red), 5 (green) and 8 (blue) of Q, multiplied by the norm of $\mathbf{r}(t)$, while the purple curve is defined by (6) with

$$\beta_0 = -1,\ \beta_1 = 3,\ \beta_1 = -2, \beta_3 = -4.$$

Figure 1 also shows the graphs of $\mathrm{Re}(\mathbf{r}(t)\,\mathbf{r}_\perp(t))$ for these four curves, which exhibit equal areas above and below the t–axis.

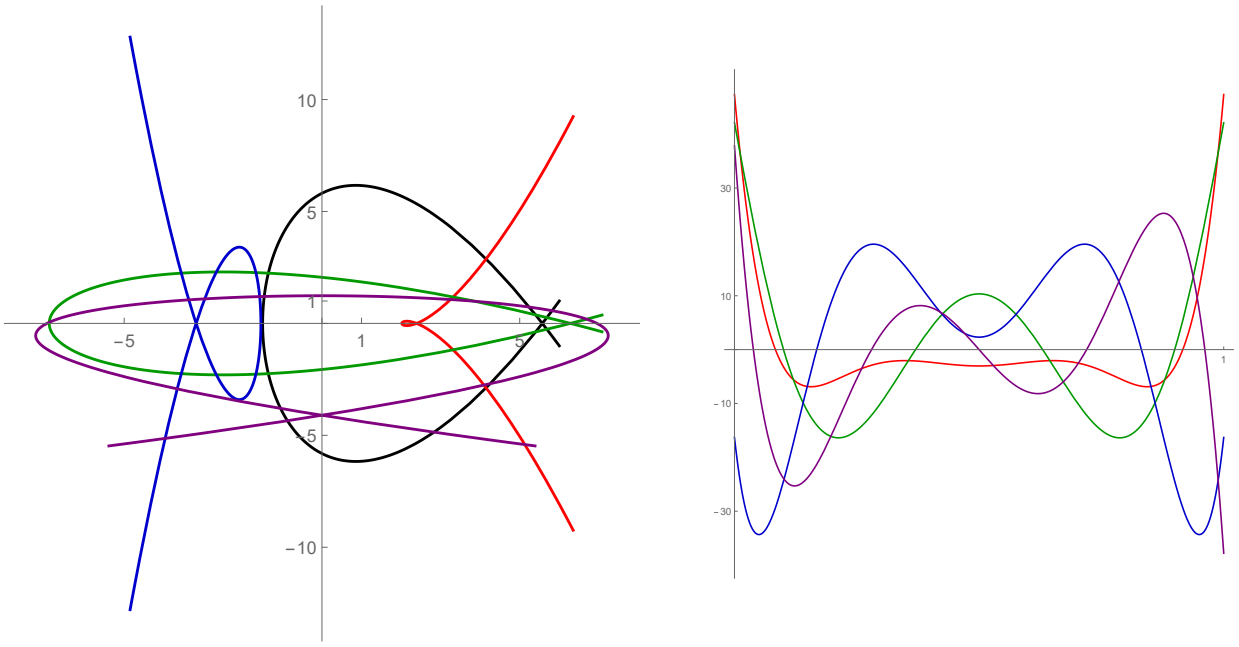

Figure 1: Left: the curve $\mathbf{r}(t)$ in Example 1 is indicated in black, and four curves $\mathbf{r}_\perp(t)$ orthogonal to it are shown in red, green, blue, and purple. Right: the graphs of $\mathrm{Re}(\mathbf{r}(t)\,\mathbf{r}_\perp(t))$ for these four curves.

Example 2. The cubic curve

$$\mathbf{r}(t) \;=\; 7\,b_1^3(t) + \frac{16}{3}\,b_2^3(t) + \mathrm{i}\left(\frac{20}{3}\,b_1^3(t) - \frac{11}{3}\,b_2^3(t) + \frac{19}{3}\,b_3^3(t)\right)$$

is a PH curve, since $\mathbf{r}'(t) = [\,5\,b_0^1(t) - 3\,b_1^1(t) + \mathrm{i}\,(2\,b_0^1(t) - 5\,b_1^1(t))\,]^2$. From its Legendre coefficients, we obtain the vector

$$\boldsymbol{a} \;=\; \left(\frac{37}{12}, \frac{7}{3}, -\frac{\sqrt{3}}{12}, \frac{13\sqrt{3}}{30}, -\frac{37\sqrt{5}}{60}, \frac{\sqrt{5}}{6}, \frac{\sqrt{7}}{28}, \frac{4\sqrt{7}}{15}\right),$$

and columns 2–8 of its QR decomposition define 7 orthogonal curves $\mathbf{r}_{\perp,k}(t)$, $k = 1, \ldots, 7$. We compute their linear combination

$$\mathbf{r}_\perp(t) \;=\; \sum_{k=1}^{7} \xi_k\,\mathbf{r}_{\perp,k}(t)\,,$$

so that $\mathbf{r}_\perp(t)$ is a PH curve. To equate the number of equations and unknowns $\xi_1, \ldots, \xi_7$ we also require $\mathbf{r}_\perp(0) = 0$, and $\mathbf{r}_\perp(t)$ to have a prescribed parametric speed, $\sigma(t) = 20 - 40\,t + 38\,t^2$.

The resulting nonlinear system has six different solutions, illustrated in Figure 2. Note that the prescribed $\sigma(t)$ implies that curves $\mathbf{r}(t)$ and $\mathbf{r}_\perp(t)$ all have the same arc length, namely 38/3.

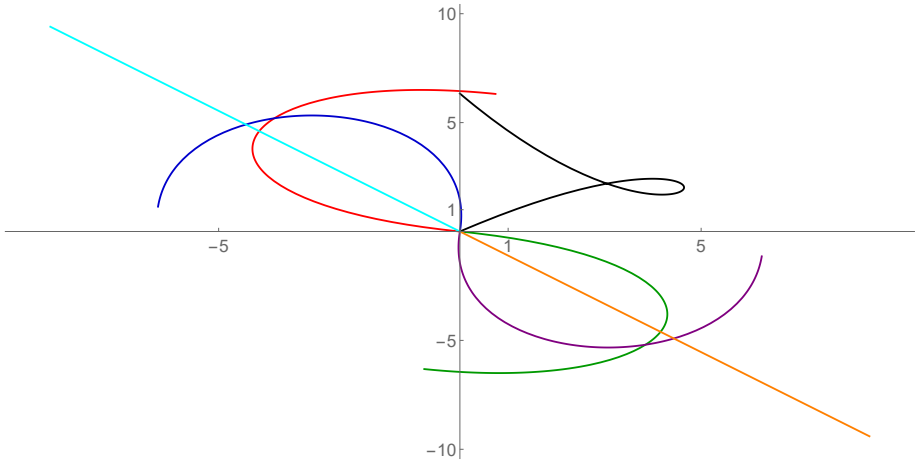

Figure 2: The cubic PH curve $\mathbf{r}(t)$ (black) in Example 2, together with the six PH curves $\mathbf{r}_\perp(t)$ orthogonal to it (shown in different colors) that possess the same start point $(0,0)$ and the same parametric speed $\sigma(t)$.

4 Planar Pythagorean-hodograph curves

Planar PH curves $\mathbf{r}(t)$ are generated from complex pre–image polynomials $\mathbf{w}(t)$ by integrating the derivative or *hodograph* $\mathbf{h}(t) := \mathbf{r}'(t) = \mathbf{w}^2(t)$. If $\mathbf{w}(t)$ is of degree m, specified in Bernstein form as

$$\mathbf{w}(t) \;=\; \sum_{k=0}^{m} \mathbf{w}_k b_k^m(t)\,, \tag{7}$$

the hodograph may be written as

$$\mathbf{h}(t) \;=\; \sum_{k=0}^{2} \mathbf{h}_k b_k^{2m}(t)\,,$$

with coefficients determined [7] by

$$\mathbf{h}_k \;=\; \sum_{j=\max(0,k-m)}^{\min(m,k)} \frac{\binom{m}{j}\binom{m}{k-j}}{\binom{2m}{k}}\, \mathbf{w}_j \mathbf{w}_{k-j}\,, \quad 0 \le k \le 2m+1\,. \tag{8}$$

The Bézier control points of the PH curve of degree $n = 2m+1$ constructed by integrating $\mathbf{r}'(t)$ are then given by

$$\mathbf{p}_{k+1} \;=\; \mathbf{p}_k + \frac{\mathbf{h}_k}{2m+1}\,, \quad k = 0, \ldots, n-1\,, \tag{9}$$

where we henceforth assume $\mathbf{p}_0 = 0$ as the integration constant.

We focus mainly on the planar PH quintics, generated from a quadratic pre–image polynomial (7), which are widely considered to be the lowest–order PH curves appropriate to free–form design applications. The control points of the Bézier form

$$\mathbf{r}(t) \;=\; \sum_{k=0}^{5} \mathbf{p}_k b_k^5(t)\,,$$

are

$$\begin{aligned}
&\mathbf{p}_1 = \mathbf{p}_0 + \frac{1}{5}\,\mathbf{w}_0^2\,, \quad \mathbf{p}_2 = \mathbf{p}_1 + \frac{1}{5}\,\mathbf{w}_0\mathbf{w}_1\,,\\
&\mathbf{p}_3 = \mathbf{p}_2 + \frac{1}{5}\,\frac{2\,\mathbf{w}_1^2 + \mathbf{w}_0\mathbf{w}_2}{3}\,,\\
&\mathbf{p}_4 = \mathbf{p}_3 + \frac{1}{5}\,\mathbf{w}_1\mathbf{w}_2\,, \quad \mathbf{p}_5 = \mathbf{p}_4 + \frac{1}{5}\,\mathbf{w}_2^2\,.
\end{aligned} \tag{10}$$

Planar PH quintics are typically constructed as solutions to a first–order Hermite interpolation problem [12] for specified end points $\mathbf{r}(0), \mathbf{r}(1)$ and end derivatives $\mathbf{r}'(0)$, $\mathbf{r}'(1)$. It is not feasible to modify their shape *a posteriori* by manipulating the control points, since this will ordinarily compromise their PH nature. Modifications that preserve the PH property of a curve should be made to its pre–image polynomial, rather than directly to the PH curve. The metric will therefore be primarily used to measure the distance between an original and modified pre–image polynomial and the PH curve it generates.

5 Perturbation of pre-image polynomials

A key application of the metric for complex polynomials is to provide a means to make "modest" shape changes to PH curves that preserve the PH property. To achieve this, modifications must be made to the pre–image polynomial. We consider perturbations $\delta\mathbf{w}(t)$ to a given pre–image polynomial $\mathbf{w}(t)$ that, for a prescribed bound Δ, satisfy

$$\text{distance}(\mathbf{w}, \mathbf{w} + \delta\mathbf{w}) \;=\; \|\delta\mathbf{w}\| \;\leq\; \Delta\,. \tag{11}$$

The perturbed pre–image polynomial determines a perturbed PH curve, with control points $\mathbf{p}_k$ displaced to $\mathbf{p}_k + \delta\mathbf{p}_k$ for $k = 1, \ldots, n$. The perturbations $\delta\mathbf{p}_k$ may be obtained by replacing $\mathbf{w}_k$

by $\mathbf{w}_k + \delta\mathbf{w}_k$ in (8) and (9), and they determine a perturbation $\delta\mathbf{r}(t)$, whose norm provides a measure of the difference between the modified and original curves.

Henceforth, we use the Legendre and Bernstein forms of both $\mathbf{w}(t)$ and $\delta\mathbf{w}(t)$ interchangeably. Whereas the former offers more concise formulations, the latter is the standard representation scheme in computer aided geometric design and offers simpler implementation of certain constraints, such as the preservation of initial/final tangent directions.

The following lemma [5] describes the transformation between these two representations, which is known to be quite numerically stable.

Lemma 1. *For a polynomial $p(t)$ of degree n expressed in the Legendre and Bernstein bases on $[\,0,1\,]$ as*

$$p(t) \;=\; \sum_{k=0}^{n} c_k L_k(t) \;=\; \sum_{j=0}^{n} d_j\, b_j^n(t)\,,$$

the coefficients $\boldsymbol{C} = (c_0,\ldots,c_n)^T$ and $\boldsymbol{D} = (d_0,\ldots,d_n)^T$ are related according to $\boldsymbol{D} = M_n\boldsymbol{C}$, where M_n is the $(n+1)\times(n+1)$ matrix with elements

$$M_{n,jk} \;=\; \frac{\sqrt{2k+1}}{\binom{n}{j}} \sum_{i=\max(0,j+k-n)}^{\min j,k} (-1)^{k+i} \binom{k}{i}\binom{k}{i}\binom{n-k}{j-i}\,, \quad 0\le j,k\le n\,,$$

whose inverse M_n^{-1} has elements

$$M_{n,jk}^{-1} \;=\; \frac{\sqrt{2j+1}}{n+j+1}\binom{n}{k}\sum_{i=0}^{j}(-1)^{i+j}\frac{\binom{j}{i}\binom{j}{i}}{\binom{n+j}{k+i}}\,, \quad 0\le j,k\le n\,.$$

Note that the columns of the matrix M_n are orthogonal.

Example 3. For the linear, quadratic, and cubic pre–image polynomials of cubic, quintic, and septic PH curves, the matrices M_n and their inverses are

$$M_1 = \begin{bmatrix} 1 & -\sqrt{3} \\ 1 & \sqrt{3} \end{bmatrix}, \quad M_1^{-1} = \begin{bmatrix} \frac{1}{2} & \frac{1}{2} \\ -\frac{\sqrt{3}}{6} & \frac{\sqrt{3}}{6} \end{bmatrix},$$

$$M_2 = \begin{bmatrix} 1 & -\sqrt{3} & \sqrt{5} \\ 1 & 0 & -2\sqrt{5} \\ 1 & \sqrt{3} & \sqrt{5} \end{bmatrix}, \quad M_2^{-1} = \begin{bmatrix} \frac{1}{3} & \frac{1}{3} & \frac{1}{3} \\ -\frac{\sqrt{3}}{6} & 0 & \frac{\sqrt{3}}{6} \\ \frac{\sqrt{5}}{30} & -\frac{\sqrt{5}}{15} & \frac{\sqrt{5}}{30} \end{bmatrix},$$

$$M_3 = \begin{bmatrix} 1 & -\sqrt{3} & \sqrt{5} & -\sqrt{7} \\ 1 & -\frac{\sqrt{3}}{3} & -\sqrt{5} & 3\sqrt{7} \\ 1 & \frac{\sqrt{3}}{3} & -\sqrt{5} & -3\sqrt{7} \\ 1 & \sqrt{3} & \sqrt{5} & \sqrt{7} \end{bmatrix}, \quad M_3^{-1} = \begin{bmatrix} \frac{1}{4} & \frac{1}{4} & \frac{1}{4} & \frac{1}{4} \\ -\frac{3\sqrt{3}}{20} & -\frac{\sqrt{3}}{20} & \frac{\sqrt{3}}{20} & \frac{3\sqrt{3}}{20} \\ \frac{\sqrt{5}}{20} & -\frac{\sqrt{5}}{20} & -\frac{\sqrt{5}}{20} & \frac{\sqrt{5}}{20} \\ -\frac{\sqrt{7}}{140} & \frac{\sqrt{7}}{140} & -\frac{3\sqrt{7}}{140} & \frac{\sqrt{7}}{140} \end{bmatrix}.$$

In the Legendre form, the pre–image polynomial (7) is expressed in terms of coefficients $\mathbf{c}_0, \ldots, \mathbf{c}_m$ as

$$\mathbf{w}(t) \;=\; \sum_{k=0}^{m} \mathbf{c}_k L_k(t)\,, \tag{12}$$

and the Bernstein coefficients can be recovered from the Legendre coefficients through the relations

$$\mathbf{w}_j \;=\; \sum_{k=0}^{m} M_{m,jk}\,\mathbf{c}_k\,, \quad j = 0, \ldots, m\,, \tag{13}$$

from which the Bézier control points (9) may be determined. The Legendre and Bernstein forms of the perturbation polynomial are

$$\delta\mathbf{w}(t) \;=\; \sum_{k=0}^{m} \delta\mathbf{c}_k L_k(t) \;=\; \sum_{j=0}^{m} \delta\mathbf{w}_j b_j^m(t)\,.$$

The relations (13) also hold for $\delta\mathbf{w}_j$ in terms of $\delta\mathbf{c}_k$, i.e.,

$$\delta\boldsymbol{W} \;=\; M_m\,\delta\boldsymbol{C}, \quad \delta\boldsymbol{W} := (\delta\mathbf{w}_0, \ldots, \delta\mathbf{w}_m)^T, \quad \delta\boldsymbol{C} := (\delta\mathbf{c}_0, \ldots, \delta\mathbf{c}_m)^T. \tag{14}$$

In the Legendre form, the norm of the perturbation $\delta\mathbf{w}(t)$ is

$$\|\delta\mathbf{w}\| \;=\; \sqrt{|\delta\mathbf{c}_0|^2 + \cdots + |\delta\mathbf{c}_m|^2} \;=\; \|\delta\boldsymbol{C}\|_2\,, \tag{15}$$

where $\|\cdot\|_2$ again denotes the standard Euclidean norm. Writing perturbation coefficients as

$$\delta\mathbf{c}_k \;=\; \rho_k \exp(\mathrm{i}\,\varphi_k), \quad k = 0, \ldots, m\,, \tag{16}$$

the inequality (11) becomes simply

$$\|\delta\mathbf{w}\| \;=\; \sqrt{\sum_{k=0}^{m} \rho_k^2} \;\le\; \Delta\,. \tag{17}$$

For perturbations of equal magnitude $\rho := \rho_0 = \cdots = \rho_m$ it further simplifies to

$$\|\delta\mathbf{w}\| \;=\; \sqrt{m+1}\,\rho \;\le\; \Delta\,, \tag{18}$$

so choosing $\rho \leq \Delta/\sqrt{m+1}$ satisfies the condition (11) for any given Δ.

In the Bernstein form $\|\delta\mathbf{w}\|$ may be expressed, using (14) and (15), as

$$\|\delta\mathbf{w}\| \;=\; \|M_m^{-1}\,\delta\boldsymbol{W}\|_2.$$

Since

$$\|M_m^{-1}\,\delta\boldsymbol{W}\|_2 \;\leq\; \|M_m^{-1}\|_2\,\|\delta\boldsymbol{W}\|_2\,,$$

where $\|M_m^{-1}\|_2$ is the matrix norm induced by the Euclidean vector norm, which is equal to the largest singular value $\sigma_{\max}\,(M_m^{-1}) \;=\; 1/\sqrt{m+1}$, any choice of coefficients $\delta\boldsymbol{W}$ such that $\|\delta\boldsymbol{W}\|_2 \leq \sqrt{m+1}\,\Delta$ ensures satisfaction of (11) for any given Δ. If we express

$$\delta\mathbf{w}_k \;=\; r_k\exp(\mathrm{i}\,\phi_k)\,, \quad k=0,\ldots,m\,, \tag{19}$$

then $\|\delta\boldsymbol{W}\|_2 = \sqrt{\sum_{k=0}^{m} r_k^2}$, and in the case of equal–magnitude perturbations, $r := r_0 = \cdots = \mathbf{r}_m$, the simple choice $r \leq \Delta$ implies that (11) holds true. However, this is just a sufficient condition. The inequality (11) can be satisfied for larger values of r by using the inequalities

$$\begin{aligned}
\|\delta\mathbf{w}\| \;&=\; \frac{\sqrt{\Phi_{01}+2}}{\sqrt{3}}\,r \leq \Delta\,,\\
\|\delta\mathbf{w}\| \;&=\; \frac{\sqrt{3\,\Phi_{01}+\Phi_{02}+3\,\Phi_{12}+8}}{\sqrt{15}}\,r \leq \Delta\,,\\
\|\delta\mathbf{w}\| \;&=\; \frac{\sqrt{10\,\Phi_{01}+4\,\Phi_{02}+\Phi_{03}+9\,\Phi_{12}+4\,\Phi_{13}+10\,\Phi_{23}+32}}{\sqrt{70}}\,r \leq \Delta\,,
\end{aligned} \tag{20}$$

for $m = 1, 2, 3$, respectively, which follow from straightforward computations using the matrices in Example 3 upon setting $\Phi_{ij} := \cos(\phi_i - \phi_j)$ for brevity. In each case, the factors multiplying r in (20) are bounded from above by 1.

5.1 Preservation of curve end tangent directions

Although the Bernstein form is more involved in terms of strictly satisfying the bound $\|\delta\mathbf{w}\| = \Delta$, it provides a simple means to preserve the directions of the curve end derivatives $\mathbf{r}'(0) = \mathbf{w}_0^2$ and $\mathbf{r}'(1) = \mathbf{w}_m^2$ by, for example, choosing $\phi_0 = \arg(\mathbf{w}_0)$ and $\phi_m = \arg(\mathbf{w}_m)$, leaving $\phi_1, \ldots, \phi_{m-1}$ and $r_0, \ldots, r_m$ as free parameters — subject to (11) and (19) — to manipulate the curve shape. On the other hand, with the Legendre form and the perturbations (16), the equality $\|\delta\mathbf{w}\| = \Delta$ can be simplify satisfied by e.g. choosing $\rho_0 = \cdots = \rho_m = \Delta/\sqrt{m+1}$, but the analogous method for preserving the end derivative directions incurs the complicated conditions

$$\arg(\mathbf{w}_0) = \arg\left[\sum_{k=0}^{m} M_{m,0k}\,\mathrm{e}^{\,\mathrm{i}\,\varphi_k}\right],\;\; \arg(\mathbf{w}_m) = \arg\left[\sum_{k=0}^{m} M_{m,mk}\,\mathrm{e}^{\,\mathrm{i}\,\varphi_k}\right]. \tag{21}$$

The following example illustrates these considerations.

Example 4. Consider the quadratic pre–image polynomial $\mathbf{w}(t)$ specified by Bernstein coefficients

$$\mathbf{w}_0 = 5 + 2\,\mathrm{i}, \quad \mathbf{w}_1 = -3 - 4\,\mathrm{i}, \quad \mathbf{w}_2 = 5 + \mathrm{i}\,,$$

with corresponding Legendre coefficients

$$\mathbf{c}_0 = \frac{7}{3} - \frac{1}{3}\,\mathrm{i}, \quad \mathbf{c}_1 = -\frac{\sqrt{3}}{6}\,\mathrm{i}, \quad \mathbf{c}_2 = \frac{8\sqrt{5}}{15} + \frac{11\sqrt{5}}{30}\,\mathrm{i}\,,$$

on which we impose the perturbations of the form (19) and (16) for $m = 2$ with equal magnitudes $r = r_0 = r_1 = r_2$ and $\rho = \rho_0 = \rho_1 = \rho_2$, satisfying (11) with equality and $\Delta = 0.25$. With the Bézier representation, the end tangents are preserved by choosing $\phi_0 = \arg(\mathbf{w}_0) = \arctan(2/5)$ and $\phi_2 = \arctan(1/5)$. For $\phi_1 = 0, \pi/4, \pi/2, 3\pi/4$, we obtain from (20) that the r values for which $\|\delta\mathbf{w}\| = 0.25$ are $r = 0.25245, 0.25661, 0.29620, 0.39083$, respectively. Figure 3 depicts the original and four modified PH quintics, all satisfying $\|\delta\mathbf{w}\| = 0.25$ — their distances from the original PH quintic are $0.29691, 0.30096, 0.29884, 0.28626$, respectively. Also shown is the envelope of the family of all possible perturbed curves with the prescribed end tangents, for $r = 0.25$. Note that all the curves have been shifted so that the centroids of their Bézier control points are coincident.

With the Legendre representation, the bound $\|\delta\mathbf{w}\| = 0.25$ is attained, for any angles $\varphi_0, \varphi_1, \varphi_2$, if and only if $\rho = 0.25/\sqrt{3}$. To also preserve the end tangent directions, these angles must be chosen (see (21)) so as to satisfy

$$\begin{aligned} \arg\left(\mathrm{e}^{\mathrm{i}\,\varphi_0} - \sqrt{3}\,\mathrm{e}^{\mathrm{i}\,\varphi_1} + \sqrt{5}\,\mathrm{e}^{\mathrm{i}\,\varphi_2}\right) &= \arctan(2/5)\,, \\ \arg\left(\mathrm{e}^{\mathrm{i}\,\varphi_0} + \sqrt{3}\,\mathrm{e}^{\mathrm{i}\,\varphi_1} + \sqrt{5}\,\mathrm{e}^{\mathrm{i}\,\varphi_2}\right) &= \arctan(1/5)\,. \end{aligned}$$

For each of the values $\varphi_0 = 0, \pi/4, \pi/2, 3\pi/4$, four distinct (φ_1, φ_2) solutions were identified, defining four different perturbations of the quintic PH curve. Figure 4 compares the original PH curve with a representative perturbed PH quintic from each of the sets of four solutions. The modified PH quintics have distances 0.19350, 0.22553, 0.23572, 0.22451 from the original PH curve. The envelope of the family of modified curves for all φ_0 values and all solutions is also shown (all the curves are shifted so that the centroids of their Bézier control points are coincident).

In the preceding discussion, the perturbations incur a *global* change in the curve. In particular, the curve end points change, which may be undesirable in common design contexts. Perturbations to the pre–image polynomial that preserve the curve end points are addressed next.

Figure 3: Left: The prescribed quintic PH curve (blue), with four instances modified using the Bernstein basis (different colors), whose pre–images satisfy $\|\delta \mathbf{w}\| = 0.25$, as described in Example 4. Right: The envelope of the family of all perturbed curves with preserved end tangent directions for $r = 0.25$.

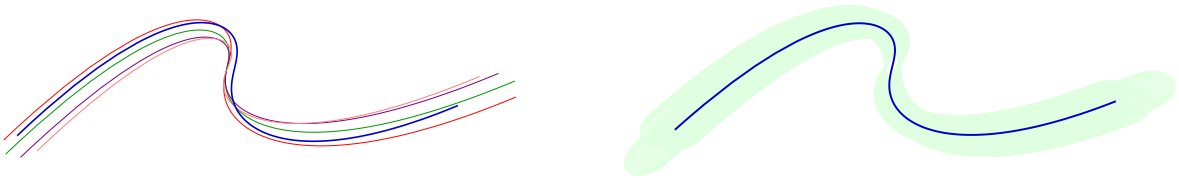

Figure 4: Left: The prescribed quintic PH curve (blue) with four instances modified using the Legendre basis (different colors), whose pre–images satisfy $\|\delta \mathbf{w}\| = 0.25$, as described in Example 4. Right: The envelope of the family of all perturbed curves with preserved end tangent directions for $\rho = 0.25/\sqrt{3}$.

5.2 Preservation of curve end points

To eliminate non–essential freedoms, it is customary to consider construction of PH curves in *canonical form* [8, 9] such that $\mathbf{r}(0) = 0$ and $\mathbf{r}(1) = 1$. The mapping of a PH curve with prescribed end points to and from canonical form can be achieved using a simple translation/rotation/scaling transformation. Thus, we confine our attention to canonical–form PH curves in investigating perturbations that preserve the curve end points. Taking $\mathbf{r}(0) = 0$ by choice of the integration constant, $\mathbf{r}(1) = 1$ is achieved through the condition

$$\int_0^1 \mathbf{r}'(t)\, \mathrm{d}t \;=\; \int_0^1 \mathbf{w}^2(t)\, \mathrm{d}t \;=\; \mathbf{r}(1) - \mathbf{r}(0) \;=\; 1\,. \tag{22}$$

In the Bernstein and Legendre representations (7) and (12) of the pre–image polynomial $\mathbf{w}(t)$, we set $\boldsymbol{C} = (\mathbf{c}_0, \ldots, \mathbf{c}_m)^T$ and $\boldsymbol{W} = (\mathbf{w}_0, \ldots, \mathbf{w}_m)^T$. As in (14), the connection between these coefficients is defined by $\boldsymbol{W} = M_m \boldsymbol{C}$ (see Lemma 1). It is easy to see that, for the Legendre form (12), the constraint (22) reduces to

$$\|\boldsymbol{C}\|_2^2 = \sum_{k=0}^{m} \mathbf{c}_k^2 \;=\; 1\,, \tag{23}$$

i.e., the Legendre coefficients correspond to points on the unit sphere in $\mathbb{C}^{m+1}$. Setting $\boldsymbol{C} = \boldsymbol{C}_R + \mathrm{i}\,\boldsymbol{C}_I$, where $\boldsymbol{C}_R, \boldsymbol{C}_I \in \mathbb{R}^{m+1}$, we note that equation (23) is satisfied if and only if

$$\|\boldsymbol{C}_R\|_2^2 - \|\boldsymbol{C}_I\|_2^2 \;=\; 1 \quad \text{and} \quad \boldsymbol{C}_R^T\,\boldsymbol{C}_I \;=\; 0\,.$$

From $\boldsymbol{C} = M_m^{-1}\boldsymbol{W}$, the constraint (22) expressed in terms of the Bernstein coefficients becomes

$$\sum_{k=0}^{m} \mathbf{c}_k^2 \;=\; \boldsymbol{C}^T\boldsymbol{C} \;=\; (M_m^{-1}\boldsymbol{W})^T(M_m^{-1}\boldsymbol{W}) \;=\; \boldsymbol{W}^T(M_m^{-1})^T M_m^{-1}\boldsymbol{W} \;=\; 1. \tag{24}$$

Setting $G_m = (M_m^{-1})^T M_m^{-1}$, we obtain for $m = 1, 2, 3$ the $(m+1)\times(m+1)$ matrices with elements $g_{m,jk}$ for $0 \le j, k \le m$ as

$$G_1 = \frac{1}{6}\begin{bmatrix} 2 & 1 \\ 1 & 2 \end{bmatrix}, \quad G_2 = \frac{1}{30}\begin{bmatrix} 6 & 3 & 1 \\ 3 & 4 & 3 \\ 1 & 3 & 6 \end{bmatrix}, \quad G_3 = \frac{1}{140}\begin{bmatrix} 20 & 10 & 4 & 1 \\ 10 & 12 & 9 & 4 \\ 4 & 9 & 12 & 10 \\ 1 & 4 & 10 & 20 \end{bmatrix},$$

and in the cases $m = 1, 2, 3$ equation (24) then reduces to

$$\begin{aligned} \mathbf{w}_0^2 + \mathbf{w}_1^2 + \mathbf{w}_1\mathbf{w}_0 \;&=\; 3, \\ 3\,\mathbf{w}_0^2 + 3\,\mathbf{w}_2^2 + 2\,\mathbf{w}_1^2 + 3\,(\mathbf{w}_0 + \mathbf{w}_2)\,\mathbf{w}_1 + \mathbf{w}_0\mathbf{w}_2 \;&=\; 15\,, \\ 10\,(\mathbf{w}_0^2 + \mathbf{w}_3^2) + 6\,(\mathbf{w}_1^2 + \mathbf{w}_2^2) + 10\,(\mathbf{w}_0\mathbf{w}_1 + \mathbf{w}_2\mathbf{w}_3) + \;4\,(\mathbf{w}_2\mathbf{w}_0 + \mathbf{w}_1\mathbf{w}_3) + \mathbf{w}_3\mathbf{w}_0 + 9\,\mathbf{w}_1\mathbf{w}_2 \;&=\; 70\,. \end{aligned}$$

To ensure that the conditions (23) and (24) are fulfilled upon substituting $\mathbf{c}_k \to \mathbf{c}_k + \delta\mathbf{c}_k$ and $\mathbf{w}_k \to \mathbf{w}_k + \delta\mathbf{w}_k$ for $k = 0, \ldots, m$, the coefficients $\delta\mathbf{c}_k$ and $\delta\mathbf{w}_k$ must satisfy

$$\sum_{k=0}^{m} \delta\mathbf{c}_k^2 + 2\sum_{k=0}^{m} \mathbf{c}_k\,\delta\mathbf{c}_k \;=\; \delta\boldsymbol{C}^T(\delta\boldsymbol{C} + 2\,\boldsymbol{C}) \;=\; 0\,, \tag{25}$$

and

$$\delta\boldsymbol{W}^T G_m(\delta\boldsymbol{W} + 2\,\boldsymbol{W}) \;=\; \sum_{j=0}^{m}\sum_{k=0}^{m} g_{m,jk}\,\delta\mathbf{w}_j\,(\delta\mathbf{w}_k + 2\,\mathbf{w}_k) \;=\; 0\,, \tag{26}$$

for the prescribed $\mathbf{c}_k$ and $\mathbf{w}_k$ values satisfying (23) and (24). In addition, the perturbations must satisfy the bounds $\|\delta\boldsymbol{C}\|_2 \le \Delta$ and $\|M_m^{-1}\delta\boldsymbol{W}\|_2 \le \Delta$. Writing $\delta\boldsymbol{C} = \delta\boldsymbol{C}_R + \mathrm{i}\,\delta\boldsymbol{C}_I$, the condition (25) is equivalent to two scalar equations in the real vectors $\delta\boldsymbol{C}_R$ and $\delta\boldsymbol{C}_I$, namely

$$\begin{aligned} \|\delta\boldsymbol{C}_R\|_2^2 - \|\delta\boldsymbol{C}_I\|_2^2 + 2\,\delta\boldsymbol{C}_R^T\boldsymbol{C}_R - 2\,\delta\boldsymbol{C}_I^T\boldsymbol{C}_I \;&=\; 0\,, \\ \delta\boldsymbol{C}_R^T\delta\boldsymbol{C}_I + \delta\boldsymbol{C}_R^T\boldsymbol{C}_I + \delta\boldsymbol{C}_I^T\boldsymbol{C}_R \;&=\; 0\,. \end{aligned} \tag{27}$$

Writing $\delta \boldsymbol{W} = \delta \boldsymbol{W}_R + \mathrm{i}\, \delta \boldsymbol{W}_I$, we have $\delta \boldsymbol{W}_R = M_m\, \delta \boldsymbol{C}_R$ and $\delta \boldsymbol{W}_I = M_m\, \delta \boldsymbol{C}_I$, so these equations can also be expressed in terms of $\delta \boldsymbol{W}_R$ and $\delta \boldsymbol{W}_I$.

This shows that in general the construction of such a perturbation $\delta \mathbf{w}$ that provides the perturbed curve to be in a canonical form and that $\|\delta \mathbf{w}\| = d \leq \Delta$ for some chosen d requires the solution of a quite complicated nonlinear system. Thus, we now propose a simple sufficient way to compute the perturbations focusing on the Legendre representation with coefficients $\delta \mathbf{c}_k$ expressed as in (16). The idea is to consider only the coefficients where all the angles are the same, i.e., $\varphi := \varphi_0 = \ldots = \varphi_m$. Then

$$\|\delta \boldsymbol{C}_R\|_2^2 - \|\delta \boldsymbol{C}_I\|_2^2 = \sum_{k=0}^{m} \rho_k^2 \, \cos(2\varphi), \quad \delta \boldsymbol{C}_R^T \delta \boldsymbol{C}_I = \frac{1}{2} \sum_{k=0}^{m} \rho_k^2 \, \sin(2\varphi),$$

so the equations (27) together with the condition

$$\|\delta \mathbf{w}\|^2 = \sum_{k=0}^{m} \rho_k^2 = d^2 \tag{28}$$

simplify to two linear equations

$$\begin{aligned} d^2 \cos(2\varphi) + 2 \sum_{k=0}^{m} \rho_k (\cos(\varphi)\, \mathrm{Re}(\mathbf{c}_k) - \sin(\varphi)\, \mathrm{Im}(\mathbf{c}_k)) = 0, \\ d^2 \sin(2\varphi) + 2 \sum_{k=0}^{m} \rho_k (\cos(\varphi)\, \mathrm{Im}(\mathbf{c}_k) + \sin(\varphi)\, \mathrm{Re}(\mathbf{c}_k)) = 0, \end{aligned} \tag{29}$$

for the radii ρ_k, $k = 0, 1, \ldots, m$, that depend on the chosen angle φ. Thus, the only nonlinear part is to satisfy (28). Next example demonstrates this construction.

Example 5. *Let us choose the pre-image polynomial of degree* 2 *with Legendre coefficients*

$$\mathbf{c}_0 = 2 - \mathrm{i}, \quad \mathbf{c}_1 = 1 + 2\ \mathrm{i}, \quad \mathbf{c}_2 = -1 + 0\ \mathrm{i},$$

which satisfy (23)*. Further, let us fix* $d = 0.1$ *and observe the perturbations of the form* (16) *with* $\varphi_0 = \cdots = \varphi_m = \varphi$ *for any* $\varphi \in (-\pi, \pi\,]$*. From* (29) *we compute*

$$\rho_1 = \frac{\rho_0}{2} - \frac{\sin(\varphi)}{400}, \quad \rho_2 = \frac{5\rho_0}{2} - \frac{\sin(\varphi)}{400} + \frac{\cos(\varphi)}{200},$$

and (28) *reduces to a quadratic equation for* ρ_0*,*

$$\frac{15}{2}\, \rho_0^2 + \frac{5\cos(\varphi)\ - 3\sin(\varphi)}{200}\, \rho_0 + \frac{\cos(2\varphi) - 2\sin(2\varphi) - 1597}{160000} = 0,$$

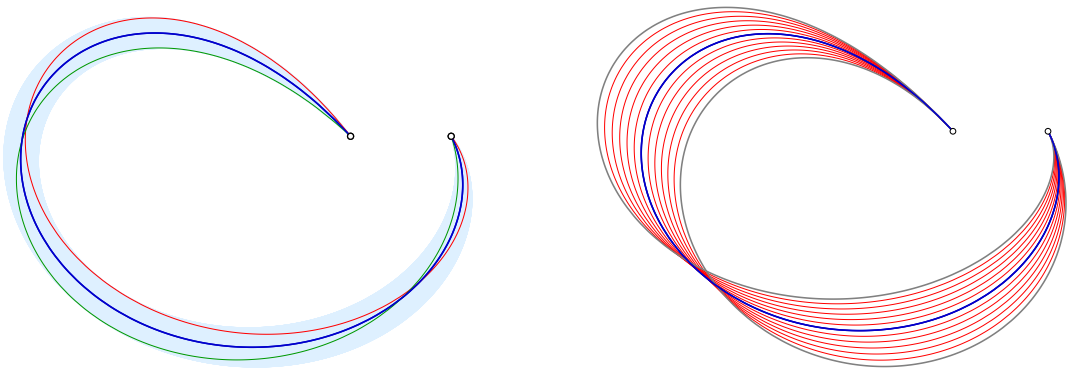

Figure 5: Left: Perturbed PH quintics (red and green) with $\|\delta \mathbf{w}\| = 0.1$ and with the same end points as the quintic PH curve (blue) from Example 5, defined by $\varphi = 0$. The envelope of all solutions for $\varphi \in (-\pi, \pi]$ is also shown (light blue). Right: The modified PH quintic curves that preserve end points and end tangent directions, as described in Example 6, as $\|\delta \mathbf{w}\|$ varies.

which has a positive discriminant for any φ. Thus there are always two admissible perturbations $\delta \mathbf{w}$, shown in Figure 5 (left) for the choice $\varphi = 0$ (red and green curve), together with the original (blue) curve and the envelope of all solutions as $\varphi \in (-\pi, \pi]$.

With the Legendre representation it is easy to construct perturbations $\delta \mathbf{w}(t)$ that preserve end points of the given curve, while the Bézier representation is more convenient for preserving end tangent directions. The constraints on the coefficients of $\delta \mathbf{w}(t)$ imposed by preserving end points and end tangent directions, coupled with the non–linear dependence of $\|\delta \mathbf{w}\|$ on those coefficients, makes it difficult to formulate schemes that guarantee an *a priori* satisfaction of the bound (11). As a practical solution for PH quintics, we consider here coefficients $\delta \mathbf{w}_0 = r \exp(\mathrm{i}\, \phi_0)$ and $\delta \mathbf{w}_2 = r \exp(\mathrm{i}\, \phi_2)$, where $\phi_0 = \arg(\mathbf{w}_0)$ and $\phi_2 = \arg(\mathbf{w}_2)$, for a prescribed r value, to preserve the end tangent directions. Preservation of the end points can then be achieved by solving the $m = 2$ instance of equation (26) for $\mathbf{w}_0, \mathbf{w}_1, \mathbf{w}_2$ values that define a canonical–form PH quintic, as a quadratic equation in $\delta \mathbf{w}_1$. Since this incurs modest computational effort, it is amenable to real–time user modification of r to ensure satisfaction of (11). However, adding the constraint $\|\delta \mathbf{w}\| = d$ for some $d \leq \Delta$ adds one nonlinear equation, but since the whole nonlinear system is algebraic, it is possible to compute all the solutions using some computer algebra system.

Example 6. Consider a canonical–form PH quintic defined by the quadratic pre–image poly-

nomial with Bernstein coefficients

$$\mathbf{w}_0 = \sqrt{2} + \frac{\sqrt{2}}{2}\,\mathrm{i}\,,$$
$$\mathbf{w}_1 = \frac{1}{4}\left(\sqrt{5(9+\sqrt{97})} - 6\sqrt{2}\right) + \left(-\frac{1}{4}\sqrt{-27+5\sqrt{97}+6\sqrt{10(\sqrt{97}-9)}}\right)\mathrm{i}\,,$$
$$\mathbf{w}_2 = \sqrt{2} + \frac{\sqrt{2}}{2}\,\mathrm{i}\,.$$

To preserve the end tangent angles $\theta_0 = \arg(\mathbf{w}_0)$ and $\theta_2 = \arg(\mathbf{w}_2)$, we set $\delta\mathbf{w}_0 = r\exp(\mathrm{i}\,\theta_0)$, $\delta\mathbf{w}_2 = r\exp(\mathrm{i}\,\theta_2)$ with some chosen r, and compute $\delta\mathbf{w}_1$ from equation (26) for $m = 2$. For $r = 0.2$ we obtain two solutions

$$\delta\mathbf{w}_1 \;=\; -0.33476348 - 0.29109547\,\mathrm{i}\,, \quad \delta\mathbf{w}_1 \;=\; -5.05586773 + 1.05285093\,\mathrm{i}\,.$$

The corresponding $\|\delta\mathbf{w}\|$ values are 0.102659, 1.802944. Figure 6 (left) shows the resulting curves. The first solution (red curve) is evidently a very reasonable modification of the original curve (blue), preserving its end points and end tangents. Although the second solution (green curve) also has this property, it exhibits tight loops — a common feature [8, 12] among the multiple solutions to PH quintics that satisfy given constraints — and is discarded on the basis of the large $\|\delta\mathbf{w}\|$ value. The perturbed curves with $\|\delta\mathbf{w}\| \le 0.25$ for $r = -0.4, -0.3, \ldots, 0.3, 0.4$ are shown (red curves) in Figure 6 (right) together with the two curves (gray) having $\|\delta\mathbf{w}\| = 0.25$, obtained for $r = -0.52962446$ and $r = 0.47220859$.

Choosing the pre-image polynomial defined in Example 5, with Bézier coefficients

$$\mathbf{w}_0 = (2-\sqrt{3}-\sqrt{5}) - (1+2\sqrt{3})\,\mathrm{i}\,,\ \mathbf{w}_1 = 2\left(1+\sqrt{5}\right) - \mathrm{i}\,,\ \mathbf{w}_2 = (2+\sqrt{3}-\sqrt{5}) + (2\sqrt{3}-1)\,\mathrm{i}$$

and different choices for r, i.e., $r = -0.5, -0.4, \ldots, 0.4, 0.5$, the modified quintic PH curves that preserve end points and end tangent directions, and satisfy $\|\delta\mathbf{w}\| \le 0.25$ are shown (red curves) in Figure 5 (right) together with the two curves (gray) having $\|\delta\mathbf{w}\| = 0.25$, obtained for $r = -0.59313245$ and $r = 0.60204179$.

6 Modification of PH curve arc lengths

The total arc length S of a planar PH curve $\mathbf{r}(t)$ is intimately related to the norm of its pre–image polynomial $\mathbf{w}(t)$, since

$$S \;=\; \int_0^1 \sigma(t)\,\mathrm{d}t \;=\; \int_0^1 |\mathbf{w}(t)|^2\,\mathrm{d}t \;=\; \|\mathbf{w}\|^2\,. \tag{30}$$

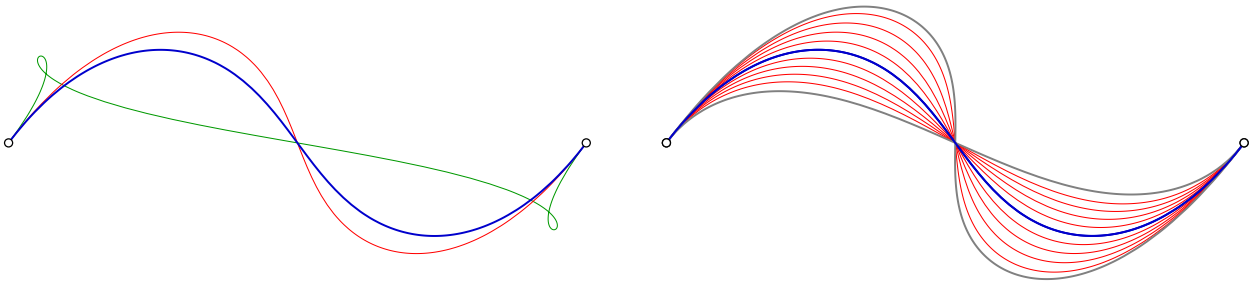

Figure 6: Left: The given canonical–form PH quintic (blue) with two modifications (red, green) that preserve the end points and tangent directions for a fixed $r = 0.2$, as described in Example 6. Right: The modified curves satisfying $\|\delta\mathbf{w}\| \leq 0.25$ as r varies.

The arc length S can be changed by a specified amount $\delta S > 0$ by choosing $\delta\mathbf{w}(t)$ to have the norm $\sqrt{\delta S}$ and to be orthogonal to $\mathbf{w}(t)$, since

$$\int_0^1 |\mathbf{w}(t) + \delta\mathbf{w}(t)|^2 \, \mathrm{d}t \;=\; \|\mathbf{w}\|^2 + \|\delta\mathbf{w}\|^2 + 2\,\mathrm{Re}(\langle \mathbf{w}, \delta\mathbf{w}\rangle)\,,$$

where $\|\mathbf{w}\|^2 = S$, $\|\delta\mathbf{w}\|^2 = \delta S$, and $\mathrm{Re}(\langle \mathbf{w}, \delta\mathbf{w}\rangle) = 0$ when $\mathbf{w}(t)$ and $\delta\mathbf{w}(t)$ are orthogonal. We focus here on the Legendre representation

$$\mathbf{w}(t) \;=\; \sum_{k=0}^{m} \mathbf{c}_k L_k(t) \quad \text{and} \quad \delta\mathbf{w}(t) \;=\; \sum_{k=0}^{m} \delta\mathbf{c}_k L_k(t)$$

of the pre–image polynomial and its perturbation. Recall the notation from Subsection 5.2. Setting $\mathbf{c}_k = c_{k,1} + \mathrm{i}\, c_{k,2}$ we form, as in Section 3, the real vectors

$$\mathbf{a} \;=\; (c_{0,1}, c_{0,2}, c_{1,1}, c_{1,2}, \ldots, c_{m,1}, c_{m,2})^T \quad \text{and} \quad \mathbf{g} \;=\; \mathbf{a} + \mathrm{sign}(c_{0,1})\|\mathbf{a}\|_2 (1, 0, \ldots, 0)^T\,. \tag{31}$$

The second through last columns of the $(2m+2)\times(2m+2)$ matrix $Q = (q_{j,k})_{j,k=1}^{2m+2}$ defined in terms of $\mathbf{a}$ and $\mathbf{g}$ defined in (31) by the formula (5) then identify the coefficients of the polynomials

$$\mathbf{b}_k(t) \;=\; \sum_{j=0}^{m} \mathbf{b}_{k,j} L_j(t)\,, \quad \mathbf{b}_{k,j} := q_{2j+1,k+1} + \mathrm{i}\, q_{2j+2,k+1}, \quad k = 1, 2, \ldots, 2m+1, \tag{32}$$

that form the orthonormal basis for degree m complex polynomials orthogonal to $\mathbf{w}(t)$ with norms $\|\mathbf{b}_k\| = 1$, $k = 1, 2, \ldots, 2m+1$. Thus, for any real values $\gamma_1, \gamma_2, \ldots, \gamma_{2m+1}$ a perturbation polynomial of the form

$$\delta\mathbf{w}(t) \;=\; \sum_{k=1}^{2m+1} \gamma_k \mathbf{b}_k(t) \tag{33}$$

is orthogonal to $\mathbf{w}(t)$ and has the norm $\|\delta\mathbf{w}\| = \sqrt{\gamma_1^2 + \gamma_2^2 + \cdots + \gamma_{2m+1}^2}$, so by assigning values $\gamma_1, \gamma_2, \ldots, \gamma_{2m+1}$ that satisfy

$$\gamma_1^2 + \gamma_2^2 + \cdots + \gamma_{2m+1}^2 \;=\; \delta S\,, \tag{34}$$

the perturbed pre–image polynomial $\mathbf{w}(t) + \delta\mathbf{w}(t)$ will generate the PH curve with arc length $S + \delta S$.

To ensure that the modified curve has the same end points as the given PH curve $\mathbf{r}(t)$, assumed to be in canonical form, $\delta\mathbf{w}(t)$ must also satisfy the condition (25), which can be reduced to the quadratic equation

$$\sum_{j,k=1}^{2m+1} \mathbf{f}_{j,k}\gamma_j\gamma_k + \sum_{k=1}^{2m+1} \mathbf{f}_k\gamma_k \;=\; 0, \quad \text{where} \quad \mathbf{f}_{j,k} := \sum_{\ell=0}^{m} \mathbf{b}_{j,\ell}\mathbf{b}_{k,\ell}, \quad \mathbf{f}_k := 2\sum_{\ell=0}^{m} \mathbf{b}_{k,\ell}\mathbf{c}_\ell, \tag{35}$$

in $\gamma_1, \ldots, \gamma_{2m+1}$. Equation (34) and the real and imaginary parts of equation (35) constitute a system of three quadratic equations for $2m+1$ factors $\gamma_1, \ldots, \gamma_{2m+1}$ in (33), which allows the user to fix $2m-2$ of them, and then solve the system using Newton–Raphson iteration or some algebraic solvers.

Remark 1. *If we denote by Q_R the sub-matrix of Q with rows $1, 3, \ldots, 2m+1$ and columns $2, 3, \ldots, 2m+2$, and by Q_I the sub-matrix of Q with rows $2, 4, \ldots, 2m+2$ and columns $2, 3, \ldots, 2m+2$, and we define the complex matrix $\boldsymbol{Q} = Q_R + \mathrm{i}\, Q_I$, then the vector $\delta\boldsymbol{C}$ of coefficients of $\delta\mathbf{w}$ can be expressed as $\delta\boldsymbol{C} = \boldsymbol{Q}\boldsymbol{\gamma}$ for $\boldsymbol{\gamma} = (\gamma_1, \gamma_2, \ldots, \gamma_{2m+1})^T$, which gives a more compact representation of* (35)*, namely*

$$\boldsymbol{\gamma}^T\boldsymbol{F}\boldsymbol{\gamma} + 2\boldsymbol{\gamma}^T\boldsymbol{Q}\boldsymbol{C} = 0, \quad \boldsymbol{F} := \boldsymbol{Q}^T\boldsymbol{Q}.$$

Example 7. Consider the PH quintic specified by the pre–image polynomial in Example 6, with arc length $S = 1.23740482$. The complex matrix $\boldsymbol{Q}$, defined in Remark 1, equals

$$\boldsymbol{Q} = \begin{pmatrix} 0.048391 + 0.998792\,\mathrm{i} & 0 & 0 & -0.148557 + 0.003707\,\mathrm{i} & -0.305920 + 0.007634\,\mathrm{i} \\ 0 & 1 & \mathrm{i} & 0 & 0 \\ 0.003707 + 0.007634\,\mathrm{i} & 0 & 0 & 0.988619 - 0.023436\,\mathrm{i} & -0.023436 + 0.951738\,\mathrm{i} \end{pmatrix}.$$

Let us choose $\delta S = 0.01$. The perturbation $\delta\mathbf{w}(t)$ is by (33) expressed with five values $\gamma_1 \ldots, \gamma_5$. We fix two of them and compute the others as the solution of equations (34)–(35). Fixing $\gamma_4 = \gamma_5 = 0$ four solutions are identified:

$$(\gamma_1, \gamma_2, \gamma_3) = (0.0047585271, \pm 0.074073623, \mp 0.067010856)\,,$$
$$(\gamma_1, \gamma_2, \gamma_3) = (-0.0047585271, \pm 0.074073623, \pm 0.067010856)\,.$$

Fixing $\gamma_2 = \gamma_3 = 0$ the sytem has only two solutions:

$$(\gamma_1, \gamma_4, \gamma_5) = (-0.032364637, 0.094555975, 0.0034202026)\,,$$
$$(\gamma_1, \gamma_4, \gamma_5) = (0.030467676, -0.094859055, 0.0085720767)\,.$$

Using these values, the Legendre coefficients of $\delta\mathbf{w}(t)$ follow from $\delta\boldsymbol{C} = \boldsymbol{Q}\boldsymbol{\gamma}$. The resulting PH quintics with increased arc length, generated by the modified pre–image polynomials $\mathbf{w}(t) + \delta\mathbf{w}(t)$, are shown in Figure 7.

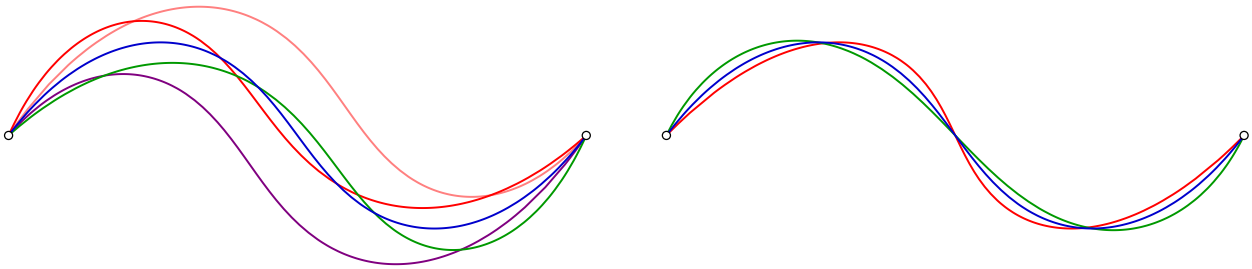

Figure 7: The PH quintic from Example 6 (blue), together with PH quintics (different colors) with arc lengths increased by $\delta S = 0.01$, sharing the same end points, computed by fixing $\gamma_4 = \gamma_5 = 0$ (left) and $\gamma_2 = \gamma_3 = 0$ (right).

Example 8. As the final example we choose the PH quintic specified by the pre–image polynomial in Example 5, with arc length $S = 11$, and follow the same steps as in the previous example. For the choice $\delta S = 0.01$ and $\gamma_4 = \gamma_5 = 0$ there are two solutions,

$$(\gamma_1, \gamma_2, \gamma_3) = (-0.068622784, 0.069792544, -0.020491812)\,,$$
$$(\gamma_1, \gamma_2, \gamma_3) = (0.068681604, -0.069717905, 0.020548745)\,,$$

shown in Figure 8 (left). Fixing $\gamma_2 = \gamma_3 = 0$ we compute

$$(\gamma_1, \gamma_4, \gamma_5) = (-0.034621641, -0.083559293, -0.042651924)\,,$$
$$(\gamma_1, \gamma_4, \gamma_5) = (0.031439019, 0.083161950, 0.045778578)\,.$$

The corresponding curves are shown in Figure 8 (right).

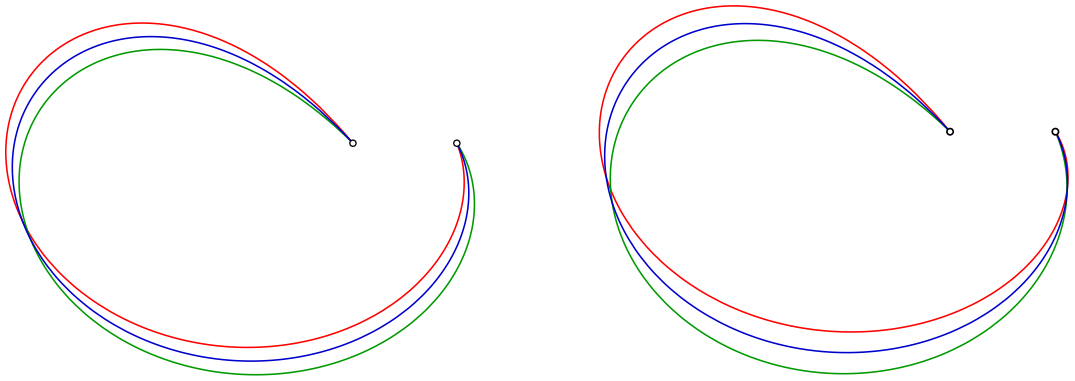

Figure 8: The PH quintic from Example 8 (blue), together with PH quintics (red, green) with arc lengths increased by $\delta S = 0.01$, sharing the same end points, computed by fixing $\gamma_4 = \gamma_5 = 0$ (left) and $\gamma_2 = \gamma_3 = 0$ (right).

7 Closure

Interpreting planar polynomial curves as complex–valued functions of a real parameter $t \in [\,0, 1\,]$ facilitates the introduction of an inner product, norm, and metric function, that permit measurement of curve magnitudes and of the distances and angles between curves. The concept of orthogonal curves is then possible, leading to a procedure to construct a basis spanning all planar curves that are orthogonal to a given planar curve.

These concepts were applied to the complex pre–image polynomials that define planar Pythagorean–hodograph (PH) curves, to develop schemes that allow bounded modifications of a given PH curve, without compromising its PH nature. Specializations of these schemes that accommodate preservation of curve end points and end tangents have also been presented, and the use of an orthogonal basis for a given PH curve pre–image polynomial to achieve a desired change in the arc length of the PH curve was demonstrated.

The methodology presented herein may also be generalized to the spatial Pythagorean–hodograph curves through the quaternion representation [3, 10] and preliminary results have already been reported in [14]. A further domain of interest concerns a possible adaptation of the methodology from curves to parametric surfaces, defined as vector quaternion polynomial functions of two parameters over triangular or rectanuglar domains.

References

[1] R. Ait–Haddou and M.–L. Mazure (2017), Sparse Pythagorean hodograph curves, *Comput. Aided Geom. Design* **55**, 84–103.

[2] G. Albrecht, C. V. Beccari, J.–C. Canonne, and L. Romani (2017), Planar Pythagorean–hodograph B–spline curves, *Comput. Aided Geom. Design* **57**, 57–77.

[3] H. I. Choi, D. S. Lee, and H. P. Moon (2002), Clifford algebra, spin representation, and rational parameterization of curves and surfaces, *Adv. Comp. Math.* **17**, 5–48.

[4] R. T. Farouki (1994), The conformal map $z \to z^2$ of the hodograph plane, *Comput. Aided Geom. Design* **11**, 363–390.

[5] R. T. Farouki (2000), Legendre–Bernstein basis transformations, *J. Comput. Appl. Math.* **119**, 145–160.

[6] R. T. Farouki (2008), *Pythagorean–Hodograph Curves: Algebra and Geometry Inseparable*, Springer, Berlin.

[7] R. T. Farouki (2012), The Bernstein polynomial basis: a centennial retrospective, *Comput. Aided Geom. Design* **29**, 379–419.

[8] R. T. Farouki (2016), Construction of G^1 planar Hermite interpolants with prescribed arc lengths, *Comput. Aided Geom. Design* **46**, 64–75.

[9] R. T. Farouki (2022), Identifying Pythagorean–hodograph curves closest to prescribed Bézier curves, *Comput. Aided Design* **149**, 103266.

[10] R. T. Farouki, M. al–Kandari, and T. Sakkalis (2002), Structural invariance of spatial Pythagorean hodographs, *Comput. Aided Geom. Design* **19**, 395–407.

[11] R. T. Farouki, M. Knez, V. Vitrih, and E. Žagar (2021), Spatial C^2 closed loops of prescribed arc length defined by Pythagorean hodograph curves, *Appl. Math. Comput.* **391**, article 125653.

[12] R. T. Farouki and C. A. Neff (1995), Hermite interpolation by Pythagorean–hodograph quintics, *Math. Comp.* **64**, 1589–1609.

[13] R. T. Farouki and T. Sakkalis (1990), Pythagorean hodographs, *IBM J. Res. Develop.* **34**, 736–752.

[14] R. T. Farouki and C. Stoppato (2024), Spatial Pythagorean hodograph curves with identical arc lengths generated by rotations of quaternion polynomials, preprint.

[15] R. W. Hamming (1986), Numerical Methods for Scientists and Engineers, Dover Publications (reprint), New York.

[16] S. H. Kim and H. P. Moon (2017), Rectifying control polygon for planar Pythagorean hodograph curves, *Comput. Aided Geom. Design* **54**, 1–14.

[17] S. H. Kim and H. P. Moon (2019), Gauss–Lobatto polygon of Pythagorean hodograph curves, *Comput. Aided Geom. Design* **74**, article 101768.

[18] E. Kreyszig (1989), *Introductory Functional Analysis with Applications*, Wiley, New York.

[19] J. Kosinka and B. Jüttler (2006), G^1 Hermite interpolation by Minkowski Pythagorean hodograph cubics, *Comput. Aided Geom. Design* **23**, 401–418.

[20] J. Kosinka and M. Lavicka (2010), On rational Minkowski Pythagorean hodograph curves, *Comput. Aided Geom. Design* **27**, 514–524.

[21] H. P. Moon (1999), Minkowski Pythagorean hodographs, *Comput. Aided Geom. Design* **16**, 739–753.

[22] H. Pottmann (1995), Rational curves and surfaces with rational offsets, *Comput. Aided Geom. Design* **12**, 175–192.

[23] H. Pottmann (1995), Curve design with rational Pythagorean–hodograph curves, *Adv. Comp. Math.* **3**, 147–170.

[24] L. Romani and F. Montagner (2019), Algebraic–trigonometric Pythagorean–hodograph space curves, *Adv. Comp. Math.* **45**, 75–98.

[25] L. Romani, L. Saini, and G. Albrecht (2014), Algebraic–trigonometric Pythagorean–hodograph curves and their use for Hermite interpolation. *Adv. Comp. Math.* **40**, 977–1010.

[26] G. Szegö (1975), *Orthogonal Polynomials*, American Mathematical Society, Providence RI.

[27] C. Zwikker (1963), *The Advanced Geometry of Plane Curves and Their Applications*, Dover Publications (reprint), New York.